Available online www.jocpr.com

Journal of Chemical and Pharmaceutical Research, 2018, 10(7): 55-62

Research Article

ISSN : 0975-7384
CODEN(USA) : JCPRC5

Synthesis and Structural characterization of Fe-doped Li-rich layered $Li(Li`_{0.21}Mn_{0.54}Ni_{0.125}Co_{0.125})O_2$ as the cathode material

Y Ezzulddin Alsayyid[1*], H Arabi[1,2] and R Etefagh[1,3,4,*]

[1]*Renewable Energies, Magnetism and Nanotechnology Research Laboratory, Departments of Physics, Faculty of Science, Ferdowsi University of Mashhad, Mashhad, Iran*

[2]*Research Center for Hydrogen Storage and Litium-Ion Battery, Faculty of Science, Ferdowsi University of Mashhad, Iran*

[3]*Department of Physics, University Campus, University of Guilan, Rasht, Iran*

[4]*Department of Physics, Payame Noor University, Tehran, Iran*

ABSTRACT

In this paper, the nanopowders of $Li(Li_{0.21}Mn_{0.54}Ni_{0.125}Co_{0.125}\text{-}x)FexO_2$ (x=0% , 0.01% ,0.025%, 0.05%, 0.075 and 0.10%) were prepared by sol-gel method, and the thermal, structural and chemical properties of the samples were investigated. These properties of samples characterized by thermogravimetric analysis (TGA), differential thermal analysis (DTA), X-ray diffraction (XRD), field-scattering microscopy (FESEM), X-ray energy spectroscopy (EDS), Transmission electron microscopy (TEM) and infrared spectroscopy (FTIR). The results of characterization were investigation. TG/DTA measurements showed weight loss in these nanopowders The XRD results reveled crystalline structures for pure and impure nanoparticles. The layerd structure remains unchanged to % 0.05 Fe but From the percentage of 0.075% to above, the additional peak, which are related to the formation of the secondary phase of $LiMn_2O4$, have been observed in the structure, which confirms the cubic structure in addition to the hexagonal. The FESEM images for pure and impure samples have shown to be agglomerated with relatively spherical and hexagonal particles of<130 nm. Image tools software was used for illustrating the distribution of particle size for pure and 0.01% Fe of impurity of nanopowders. The results of TEM revealed that with the presence of iron, the size of the particles is larger than pure nanoparticles and the range of 50-150 nm. In infrared spectroscopy (FTIR), the connection bonds and chemical elements used in these nanopowders have been investigated.

Key words: Lithium-ion battery; Cathode; Sol gel; Doping; Nanoparticles

---

INTRODUCTION

During the past decades, lithium ion batteries are receiving considerable attention as power source for electric vehicles (EVS), hybrid electric vehicles (HEVS), and large electric power tools [1-8]. In a recent period of time, layered lithium-rich materials $xLi_2MnO_3(1\text{-}x)LiMO_2$(M=Co, Ni, $Mn_{1/2}Ni_{1/2}$, $Mn_{1/3}Ni_{1/3}Co_{1/3}$, etc.) are being intensively studied for better cathode materials owning to their high capacity (>200 mAh/g) and low cost in comparison with LiCoO2 and LiFePO4 [9,10]. Among all the cathode materials of LIBs, the $xLi[Li_{1/3}Mn_{2/3}]O_2\cdot(1\text{-}x)LiMO_2$ (M=Mn, Co, Ni, etc.) is a promising material because of its high reversible capacity following an "activation" process [11-13].

Commercially applied $LiCoO_2$ cathode has benefits of easy synthesis and excellent lithium ion mobility though challenging subject of stability, achieving practical capacities, and environmental risks need to be addressed. The

layer-structured rhombohedral $LiMnO_2$ ($R\bar{3}m$) attracts interest as a potential cathode due to its cost effectiveness and relatively high capacity, but it exhibits severe capacity fading during extended cycling. More precisely, its discharge behavior during electrochemical cycling needs significant improvement. [14]

Doping has also successfully been used for improving Li-rich layered materials [15-17].The transition element in the oxide materials can be substituted by metal elements such as Al [18], Zr [19], Mo [20], Fe [21] and those doped materials show higher cyclic performance and structural stability surface modification, i.e., The sol-gel method among the various methods of synthesis, due to being provided the small particles. This method is easy and the availability of the synthesis is preferable to other methods. In this paper, undoped and doped nanopowders of $Li(Li_{0.21}Mn_{0.54}Ni_{0.125}Co_{0.125}\text{-}x)FexO_2$ were prepared with different percentages of Fe impurity by sol-gel method. TGA, XRD, FESEM, TEM and FTIR were carried out to characterize the thermal, structural and chemical properties of the materials for detailed investigation.

EXPERIMENTAL SECTION

Preparation of Materials

$Li(Li_{0.21}Mn_{0.54}Ni_{0.125}Co_{0.125}\text{-}x)FexO_2$ nanopowders for (x=0%, 0.01%, 0.25%, 0.05%, 0.075% and 0.10%) were prepared with the precursors of pristine and Fe-doped samples from pure materials of $CoN_2O_6.4H_2O$, $NiN_2O_6.6H_2O$, $C_4H_6MnO_4.4H_2O$, $Li(NO_3)$ and $Fe(NO_3)_3.9H_2O$ by sol-gel method in which citric acid was used as a chelating agent as the synthesis method. Firstly mixture was dissolved in to aqueous solutions, and then citric acid was dropped slowly into aqueous solution under stirring at 75-80°C until gel-like was obtained. The molar ratio of citric acid to total metal ions was unity. The gel was dried at 120°C in vacuum oven for 12 hour. The resulting gel precursor was decomposed at 500°C for 5 hour in air to eliminate the organic substances. The decomposed powders heated at 850°C for 6 hour. The crystal structure of the as-prepared $Li(Li_{0.21}Mn_{0.54}Ni_{0.125}Co_{0.125}\text{-}x)FexO_2$ powders were characterized by The TG/DTA analysis for pure nanopowders was performed on an STA PT1600 TG/DTA (LINSEIS) using a heating rate of 10°C/min in air. XRD with a D8 Advance Bruker YT diffractometer using CuKα radiation in the 2θ range of 10° and 80°. The size and morphology of the sample was investigated using FESEM performed on MIRA3TESCAN-XMU microscope equipped with a Thermo NORAN system 6 X-Ray microanalysis system supported by a NanoTrace LN-Cooled Si(Li) detector for Energy-dispersive X-ray Spectroscopy (EDS) analysis. The TEM analysis for nanopowders was performed on an (Leo912 AB). The infrared spectra were recorded using Fourier-transformed infrared spectrophotometer (AVATAR 370, Thermo Nicolet).

RESULT AND DISCUSSION

Thermogravimetric Analysis

In order to verify the mass changes of these powders in the sol-gel method were used figure the TG/DTA curves showed in Figure 1a and 1b for the pure and doped with Fe (0.025%) of nanopowders dry gel. For a pure sample The weak endothermic peak at about 280°C in the DTA curves of pure gel, which corresponds to a weight loss of 15% in the TG curve, is for the removal of residual water molecules. At the temperatures of 300-450°C a weight loss of 45% is detected, which accompanies a strong exothermic peak at 320°C. This weight loss as to the decomposition and combustion of clathrate and completed in 480°C.

With the presence of impurity of Fe in pure crystals, these curves are almost identical but an exothermic peak of about 180°C has been seen, that possibly related to the decomposition of hydroxyl group in these powders. The second weight loss is probably due to the formation of the $Li(Li_{0.21}Mn_{0.54}Ni_{0.125}Co_{0.125}\text{-}x)FexO_2$ crystal in 450-500°C Therefore, in the next one experiment in pure and impure of nanopowder the pre-calcinations temperature was selected at 500°C [22].

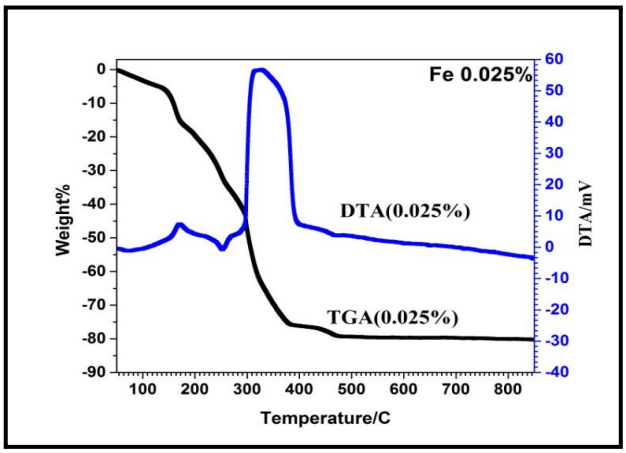

(a)

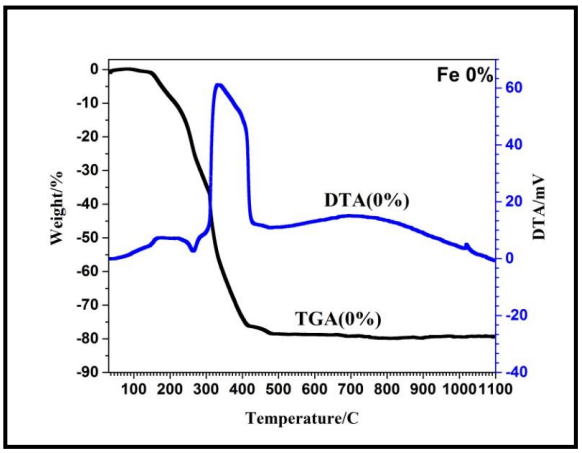

(b)

Figure 1: TG/DTA curves for a) pure dry gel b) doped with 0.025% Fe

Structural Properties

X-ray diffraction analysis:

The phase analysis and structure was conducted by the X-ray diffractometry and the resultant diffractograms are shown in Figure 2a and 2b.

Figure 2a shows nanopowders doped with 0.01% and 0.10% Fe at pre-calcinations temperature of 500°C. As shown in this figure, the main structure of the substance is not formed and the phase of this nanopowder is formed lithium manganese oxide ($Li_{14}Mn_5O_{12}$). The XRD patterns of the pristine and with impurity of Fe (0.01, 0.025, 0.05, 0.075 and 0.10%) nanopowders are shown in Figure 2b. The structure of pure and doped with Fe reveled good crystallinity with Preferred Peaks of (003) and (104). All the reflection peaks indicate that the samples have standard α-$NaFeO_2$ layered structure with the space group R-3m, except that the weak peaks in the 2θ range of 20–25° identified as the (020) and (110) reflection are attributed to the monoclinic Li_2MnO_3 phase (C2/m space group) [22]. The layerd structure remains unchanged to % 0.05 Fe but From the percentage of 0.075% to above, the additional peak, which are related to the formation of the secondary phase of $LiMn_2O_4$, have been observed in the structure, which confirms the cubic structure in addition to the hexagonal. [11,12]. the diffraction patterns show clear splitting of the hexagonal characteristic doublets of (006)/(102) and (108)/(110); and formation of cation ordered phase and indicate the good structure of layered oxides [23].

All diffraction peaks are sharp and well-defined, suggesting that the prepared samples are well-crystallized. Their crystal sizes calculated from the refection peaks of (003) by using the Scherrer equation and williamson hall and these results shows in the Table 1.

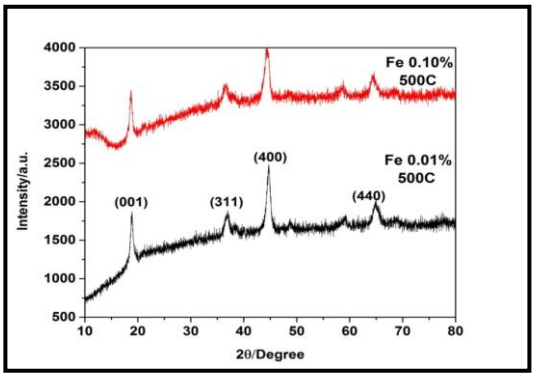

(a)

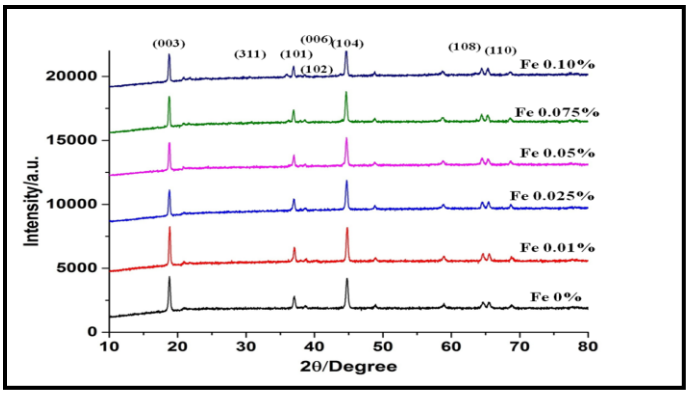

(b)

Figure 2: XRD patterns of $Li(Li_{0.21}Mn_{0.54}Ni_{0.125}Co_{0.125}\text{-}x)FexO_2$ with Fe a) (0.01% and 0.10%) calcinated at temperature of 500°C b) (x=0% to 0.10%) calcinated at temperature of 850°C

Table 1: The FWHM values for of (Li0.21Mn0.54Ni0.125Co0.125-x)FexO2

nanopowder	Compound	FWHM	D(hkl)	DW-H	ε	I/I0
pure	00-027-1252 Lithium Manganese Oxide (Li_2MnO_3) 01-087-1564 Lithium Nickel Cobalt Oxide	0.302	29.4nm	36.19nm	0.096	1.11
Fe 0.01%	00-027-1252 Lithium Manganese Oxide (Li_2MnO_3) 01-087-1564 Lithium Nickel Cobalt Oxide	0.26	34nm	72.38nm	0.08	1.11
Fe 0.025%	00-027-1252 Lithium Manganese Oxide (Li_2MnO_3) 01-087-1564 Lithium Nickel Cobalt Oxide	0.278	32.1nm	48.25nm	0.07	0.9
Fe 0.05%	00-027-1252 Lithium Manganese Oxide (Li_2MnO_3) 01-087-1564 Lithium Nickel Cobalt Oxide	0.255	32.8nm	72.38nm	0.1	1.01
Fe 0.075%	00-027-1252 Lithium Manganese Oxide (Li_2MnO_3) 01-087-1564 Lithium Nickel Cobalt Oxide Lithium Manganese Oxide $LiMn_2O_4$	0.263	33.6nm	48.28nm	0.061	1.05
Fe 0.10%	00-027-1252 Lithium Manganese Oxide (Li_2MnO_3) 01-087-1564 Lithium Nickel Cobalt Oxide Lithium Manganese Oxide $LiMn_2O_4$	0.263	39.9nm	51.70nm	0.1	1

The morphologies of the layered composites before and after Fe modification are revealed in Figure 3. It is found that the Fe-doping does not change their morphologies and all the pure and impure with Fe materials have a similar morphology and it can be seen that the as-prepared homogeneous nanoparticles have a nearly spherical and

hexagonal morphology with the size in the range of ≤120nm which would simplify the intercalate and deintercalate process for Li+ and improve ion conductivity and rate performance.

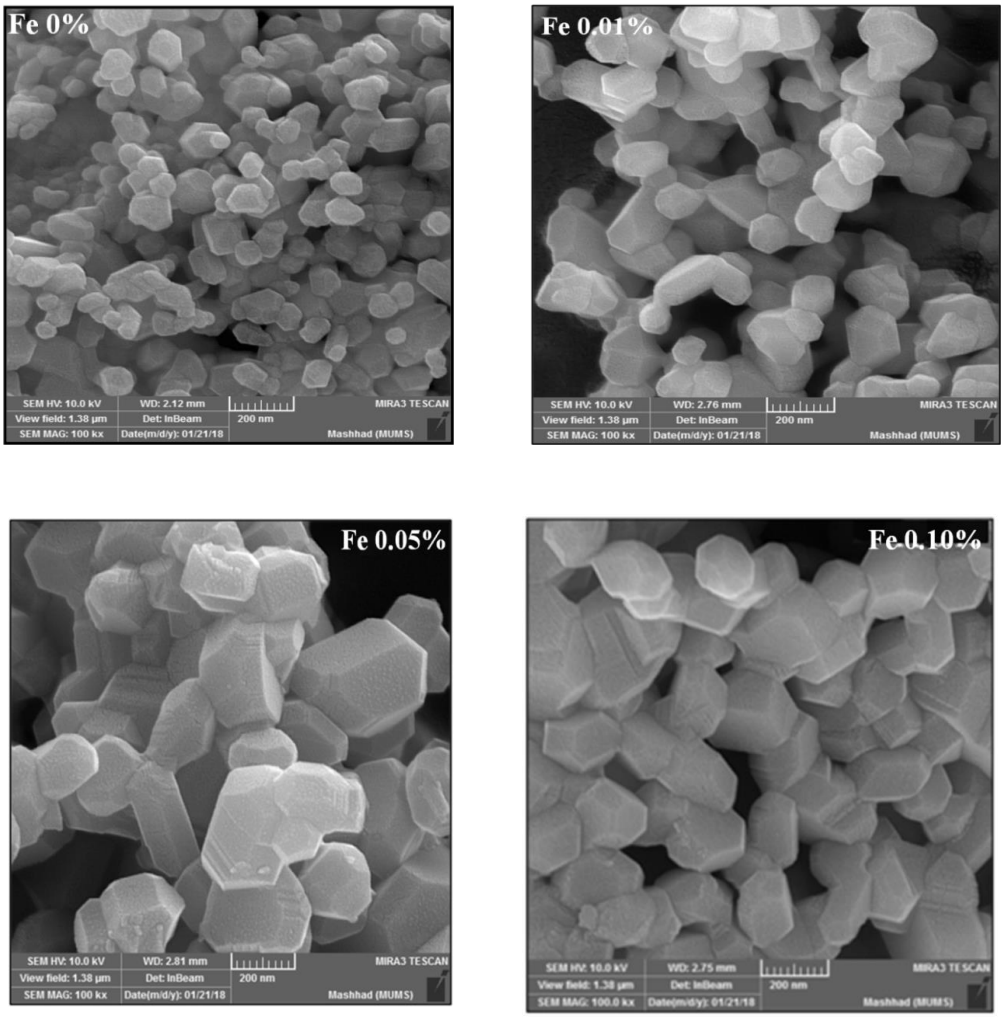

Figure 3: FESEM images of a) pure nanopowders, b) Fe 0.01, c) Fe 0.05, d) Fe 0.10

Image tools software was used for illustrating the distribution of particle size for pure and 0.01% Fe of impurity of nanopowders and showed in Figure 4. Particles of distribution for pure nanopowders are observed in the range of 50nm. By adding the impurity Fe, the particle size and distribution are increase and within the range of 60-120nm, and with the adding of the impurities, the particle size has increased.

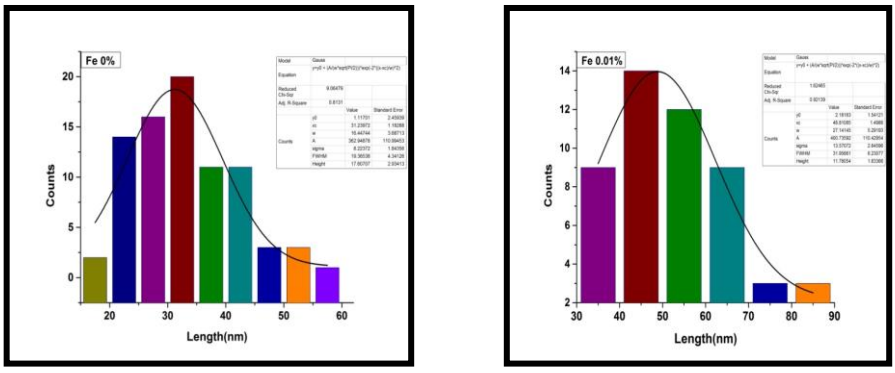

Figure 4: Particles of distribution for Li(Li0.21Mn0.54Ni0.125Co0.125-x)FexO2 nanopowders for (x=0 and 0.01%)

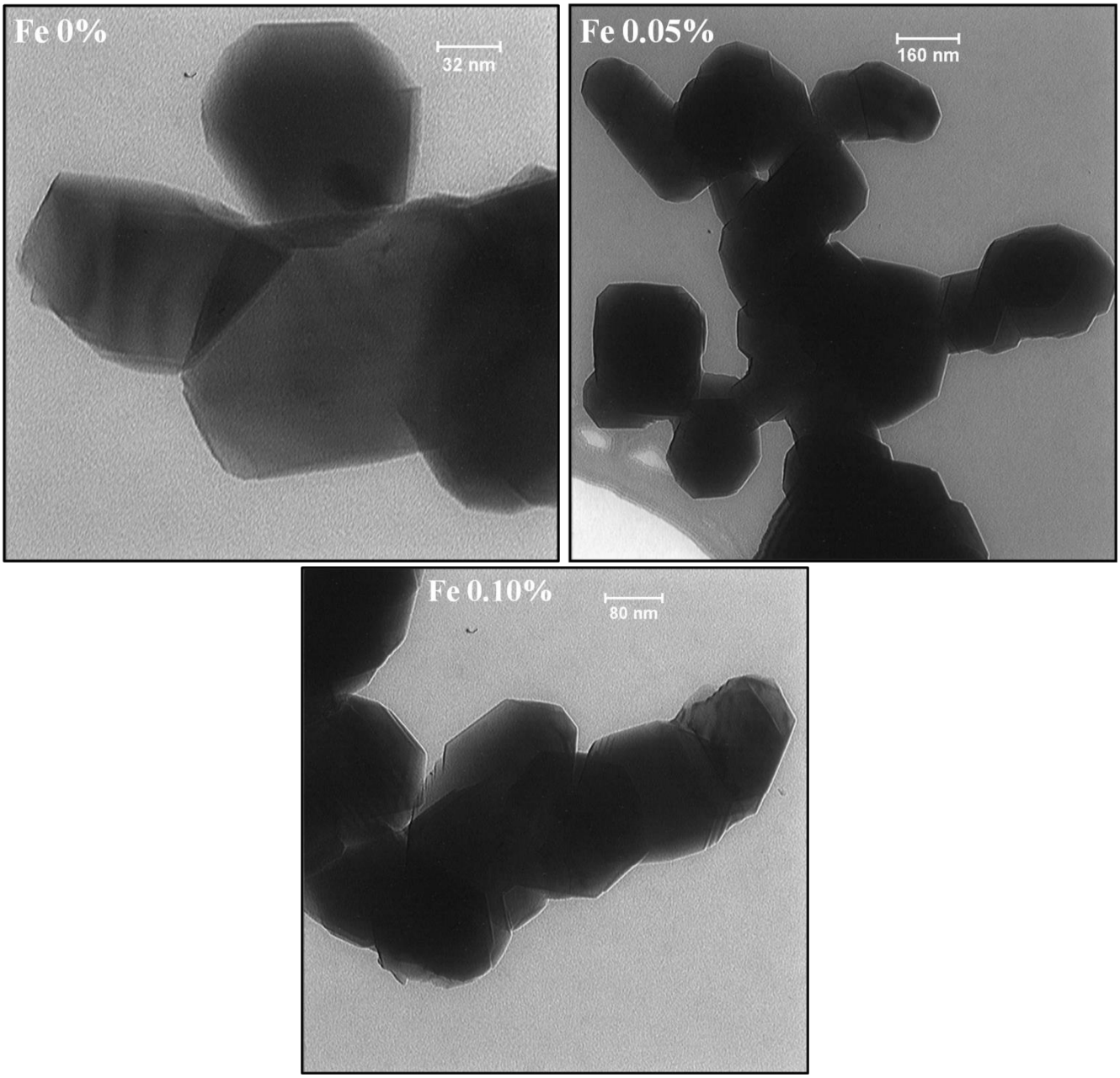

Figure 5: TEM images for Li(Li0.21Mn0.54Ni0.125Co0.125-x)FexO2 nanopowders (x=0%, 0.05% and 0.10%)

The sizes of pure and impure nanoparticels with Fe 0.05% and Fe 0.10% studied by TEM and are shown in Figure 5. TEM study provided useful information regarding the integrated structure of the Fe doped pristine material. The particles size of pure materials in the range of 50–120 nm. The particles size seems to increase with added Fe doping upon 0.10%.

In order to invest the vibrational motion of molecules and multi-atomic ions of pure powders in temperature of 120°C in vacuum aven, 500°C and 850°C, infrared spectroscopy was used based on radiation absorption. The results

of the FTIR spectroscopy for nanopowders of pure and doped with Fe 0.01% and 0.10% in temperature of 500C between wavelengths of 4000-500 Cm-1 are shown in Figure 6a and 6b.

As can be seen in Figure 6a in temperature of 850C, for pure nanopowders one peak at 3297.76 Cm-1, is the fingerprint of hydration in the collected powder. Two peaks at 1486.95 Cm-1 and 1436.40 Cm-1 reveled Li_2CO_3 and the groups of CH2 and CH3. Peaks below 1500 Cm-1 confirm the presence of metal oxygen in vibration frequencies [24]. In Figure 6b Three peaks in the region 1646.31, 1384.22 and 1867.47 Cm-1 are observed with the addition of impurities in 0.01% Fe, respectively, that corresponding to CH3OCO2Li, CH2-CH3 and (CO3)-2, with impurities added up to 0.10% peak in region 1646.31Cm-1 It has been eliminated[25,26].

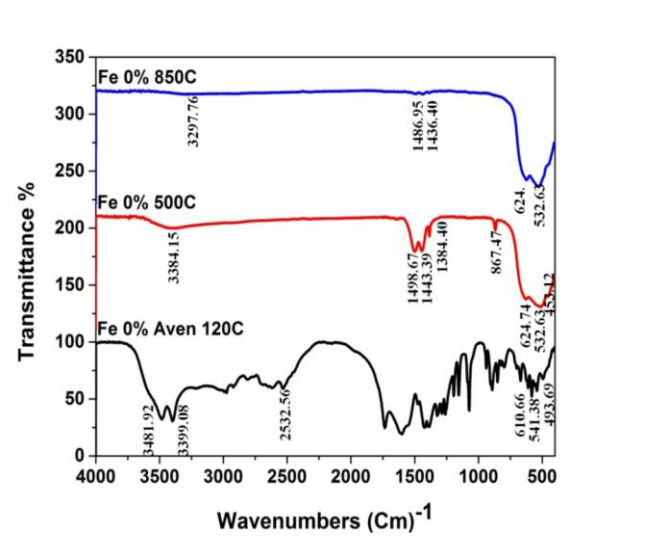

(a)

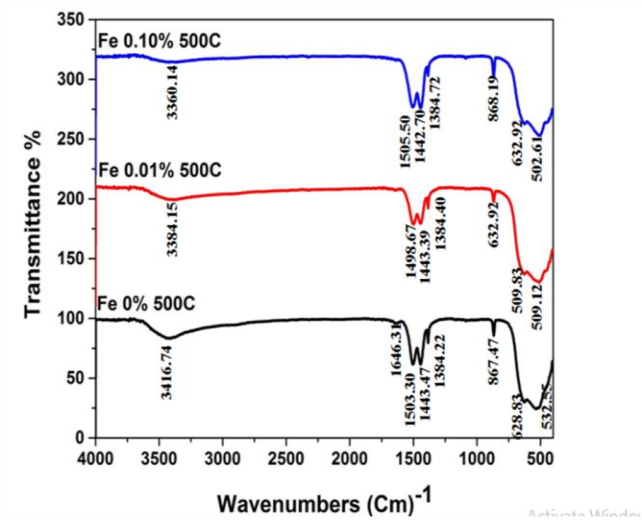

(b)

Figure6: FTIR spectra of $Li(Li_{0.21}Mn_{0.54}Ni_{0.125}Co_{0.125}-x)Fe_xO_2$ nanopowders a) pure in temperature of 120°C vacuum aven, 500°C and 850°C b) doped with 0.01% and 0.10% Fe in 500°C

CONCLUSION

In this paper we have reported the synthesis of nanocrystalline cathode layered Li(Li0.21Mn0.54Ni0.125Co0.125-X)FexO2 with different percents Fe (x=0.01%, 0.025%, 0.05%, 0.075% and 0.10%) by sol-gel method using citric acid as the chelating agent. XRD, FESEM, TEM, FTIR and TG/DTA were employed to study the structural, chemical and thermal properties of prepared nanopowders. The structural results for pure and impure nanopowders showed the single phases layered with the super lattice structure originating from the monoclinic Li_2MnO_3 and the as-prepared pure and impure of nanopowders have a nearly hexagonal morphology with an average diameter of approximately 40-120 nm in FESEM analysis. With increases impurity Fe the average size of nanoparticles are increased. TG/DTA measurement for pure nanopowders showed between 300–500°C, the weight loss of 45% is attributed to the thermal decomposition of the ingredients to form $Li(Li_{0.21}Mn_{0.54}Ni_{0.125}Co_{0.125})O2$ and with increase Fe doped in structure. FTIR spectra of $Li(Li_{0.21}Mn_{0.54}Ni_{0.125}Co_{0.125})FexO_2$ nanopowders (for x=0% in temperature of 120C in vacuum aven, 500C and calcinated at of 850°C also (for x= 0.01% and 0.10% Fe in 500C showed Peaks below 1500Cm-1 confirm the presence of metal oxygen due to vibration frequencies. Finally, this first study is helpful for the production of $Li(Li_{0.21}Mn_{0.54}Ni_{0.125}Co_{0.125}-x)FexO_2$ nanopowders with different percents as a cathode material for rechargeable lithium-ion batteries.

REFRENCES

[1] Lu Z; Macneil DD; Dahn JR. *Electrochemical Solid-State Lett*. **2001**, 34, 91.
[2] Croguennec L; Bains J; Breger J, Tessier C, Biensan P. *J Power Sources*. 2011, 158, 665.
[3] Zhou LZ; Xu QJ; Liu MS; Jin X. *S. State Lonics*. **2013**, 245, 135.
[4] Liu H; Wang Y; Li L; Wang K; Hosono E; Zhou H. *J Materials Chemistry*. **2009,** 19, 7889.
[5] Liu H; Wang Y; Wang K; Hosono E; Zhou H. *J Materials Chemistry*. **2009**, 19, 2839.
[6] Li DC; Muta T; Zhang LQ; Yoshio M; Noguchi H. *J Power Sources*. **2004,** 132,152.
[7] Li DC; Noguchi; Yoshio M, *Electrochimica Acta*. **2004,** 50, 428.
[8] Larson AC; Dreele RB; Dreele V. *L Alamos Natl Lab*. **1994,** 86, 748.
[9] Jin X; Xu Q; Liu H; Yuan X; Xia Y. *Electrochimica Acta*. 2014, 136, 19.
[10] Lu Z; Dahn JR. *J Electrochem Soc.* **2002,** 49, 815.
[11] Gong ZL; Liu HS; Guo XJ; Zhang ZR; Yang Y. *J Power Sources*. **2004**, 136 141.
[12] Liu X; Huang T; Yu A. *Electrochimica Acta*. **2014,** 133, 556.
[13] Zang C; Ding X; Wang XC; Wen ZY; Chen CH. *Electrochimica Acta*. **2015**, 168.
[14] Croguennec L; Deniard P; Brec R. *J Electrochem Soc.* **1997**, 144, 3323-3330.
[15] Nayak PK; Grinblat J; Levi M; Aurbach D. *Electrochim Acta.* **2014,** 137, 546.
[16] Wang D; Huang V; Huo ZhQ; L Chen. *Electrochim Acta.* **2013,** 107, 461.
[17] Yamamoto S; Noguchi H; Zhao WW. *Power Sources.* **2015,** 278,76.
[18] Fang H; H Yi C Hu; Yang B; Yao Y; Ma W. *Electrochimica Acta.* **2012,** 71, 266.
[19] Jeong KH; Ha HW; Yun NJ; Hong MZ; Kim K. *Electrochimica Acta.* **2005**, 50, 5349.
[20] Park JH; Lim J; Yoon J; Park KS; Gim J; Song J. *Dalton Trans*. **2012,** 41, 3053.
[21] Wang D, Huang Y, Huo Z, Chen L. *Electrochimica Acta.* **2013**, 107, 461.
[22] Hao WJ; Zhan HH; Chen H; Wang YH; Tan QQ; Su FB. *Particuology*, **2013,** 33.
[23] Wei X; Yang P; Li H; Wang S; Xing Y; Liu X; Zhang S. *RSC Adv*. **2017,** 7.
[24] Haik O; Leifer N; Fromovich Z; Zinigrad E; Markovsky B; Larush L; Goffer Y; Goobes G; Aurbach D *J Electrochem Soc.* **2010,** 157, 10.
[25] Lu Z; Beaulieu LY; Donaberger RA; Thomas CL; Dahn JR. *J Electrochem Soc*. **2002,** 149, 778-791.
[26] Robertson AD; Bruce PG. *Chem Mater.* **2003,** 15, 1984-1992.